Proceedings of the 9th International Conference on Civil Structural and Transportation Engineering (ICCSTE 2024)
Chestnut Conference Centre - University of Toronto, Toronto, Canada – June 13-15, 2024
Paper No. 251
DOI: 10.11159/iccste24.251

Numerical Investigation on Buckling Response of Cylindrical Steel Storage Tanks Under Static Loading

Shafqat Ullah[1], Iraj H. P Mamaghani [1]
[1]University of North Dakota
Department of Civil Engineering
243 Centennial Drive, Stop 8115, Grand Forks 58203, USA
shafqat.ullah@und.edu; iraj.mamaghani@und.edu

Abstract **–** Cylindrical steel shells find extensive use in critical structures such as submarines, launch vehicles, and industrial facilities, highlighting the paramount importance of their stability performance. This study delves into the buckling response of these structures, considering various factors including imperfections, loading conditions, and material behavior. Specifically, we investigate the buckling behavior of both perfect steel models and those reinforced with carbon-fiber-reinforced polymers (CFRP) under axial and uniform external pressure. Employing linear and nonlinear analysis techniques using ABAQUS software, we evaluate the structural response and compare results with experimental data and theoretical predictions. Our findings demonstrate good agreement among finite element analysis (FEA), test results, and theoretical calculations. Moreover, we explore the influence of lay-up orientation on buckling resistance, highlighting the significance of fiber arrangement in CFRP reinforcement. Additionally, we analyse the deformation and stress distribution in cylindrical steel tanks subjected to hydrostatic pressure, revealing that maximum stresses occur at the bottom where liquid pressure is highest. These insights contribute to a deeper understanding of cylindrical steel shell behavior and have practical implications for enhancing their buckling capacity and structural integrity.

Keywords**:** Linear and Non-Linear Buckling Analysis, Cylindrical Steel Shell, CFRP Strengthening, Finite Element Analysis, ABAQUS Software

1. Introduction

The cylindrical steel storage tanks are important structural components in industries, power plants, refineries, and agricultural facilities. These tanks are mainly used to store liquids including water, liquified natural gas (LNG), petrochemicals, and other hazardous substances[1]. Based on previous studies, steel storage tanks compared to concrete tanks are more prone to buckling and damage during wind loading, uniform external pressure as well as seismic events. The buckling analysis is divided into bifurcation and load-deflection analysis as shown in Figure 1[2]. The buckling (bifurcation) takes place when the maximum axial stresses reach the buckling stresses.

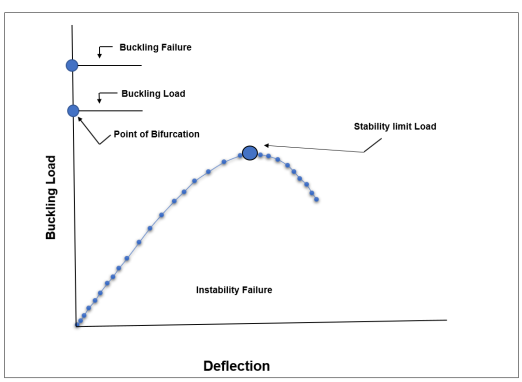

Fig. 1: Load Vs Deflection curve- Buckling analysis

Buckling in cylindrical steel tanks can be categorized in the form of elephant foot (elastic-plastic) buckling, which is in the form of an outward bulge near the base of the tanks caused by excessive axial compressive stress and diamond shape buckling as illustrated in Fig 2(a), (b) and (c) respectively [3-4].

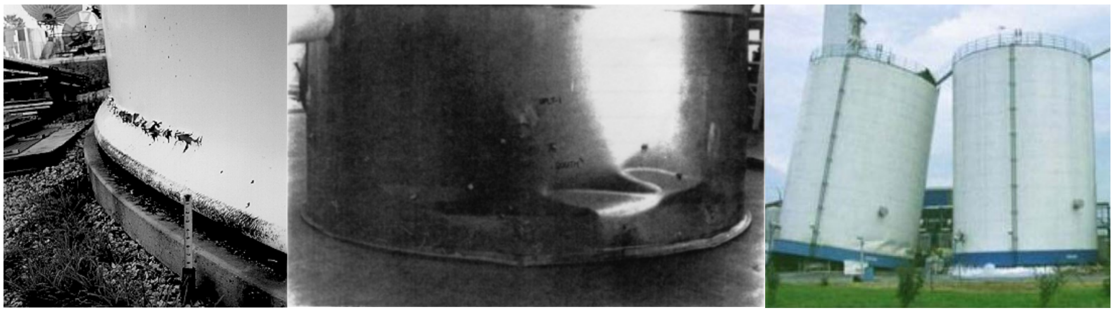

(a) (b) (b)

Fig. 2: (a) Elephant foot buckling of the tank during an earthquake (Haroun et al [2005] and (b) Diamond-shaped buckling and (c): overturning of storage tanks during earthquake (Burati [2010].

Tabish and Mamaghani [5] conducted numerical studies on cylindrical steel tanks under static loading. the authors investigated the effects of different H/D and D/t ratio on buckling resistance of the cylindrical empty tanks. Tabish and Mamaghani [6] numerically investigated the linear and non-linear buckling behavior of cylindrical perfect and imperfect shells under external pressure. Aghajari et al., [7] presented a detailed experimental and numerical investigation of the buckling response of cylindrical shells with different shell thicknesses when subjected to external uniform pressure. Wang et al., [8] investigated the buckling response of the cylindrical tanks under the influence of axial compression loading as well as internal pressure. Researchers such as Greenberg and Stavsky [9] investigated the buckling resistance of composite cylindrical shells subjected to static loading. Nowadays, researchers are investigating the effects of carbon fiber-reinforced polymers (CFRP) on the buckling strength of cylindrical steel shells under different loading conditions.

This study presents a detailed finite element analysis (FEA) study on the buckling response of cylindrical steel tanks with and without CFRP strengthening subjected to axial loading, uniform external pressure as well as hydrostatic loading. The results from the existing literature are validated to substantiate the accuracy of the FEA ABAQUS software.

2. Finite Element Modeling Approach

This research study investigates the buckling response of cylindrical steel tanks under different loading conditions such as axial loading, uniform external pressure, and earthquake loading. finite element analysis (FEA) using commercial software ABAQUS is conducted to evaluate the buckling load using linear and non-linear buckling analysis. Initially, the cylindrical steel shells (unreinforced) are considered for linear buckling analysis and the FE results are compared with both test as well as theoretical solutions. The detailed study of different cylindrical tank models is discussed in section 2.1.

2.1. Linear Buckling Analysis (LBA) for Cylindrical Shells

The existing test results in the literature are used to validate and check the accuracy of the FEA ABAQUS software. A total of 3 cylindrical steel tank models are considered for static buckling analysis and the results of FE models are compared with the experimental results as well as theoretical solutions. Model-1 is considered a perfect-unreinforced cylindrical shell and is subjected to external uniform pressure. The geometry and material properties of the model are given in Table 1.

Table 1: Geometry and material properties of the cylindrical steel shells

S. No	Geometric Properties			Material Properties		
	Height (H) mm	Radius (R) mm	Thickness (t) mm	Young's modulus (E) MPa	Yield stress MPa	Poison's ratio v
01	1250	500	1.00	210	198.8	0.29

Different mesh sizes were used for the cylindrical shell and their effects on buckling load are investigated. Finally, a 14 mm mesh size with a total of 23136 elements is adopted for eigenvalue buckling analysis. Simply supported condition at the top and bottom of the cylindrical shell is used and subjected to external uniform pressure. Figures 3 (a), and (b) represent the meshing and boundary conditions of the cylindrical shell respectively.

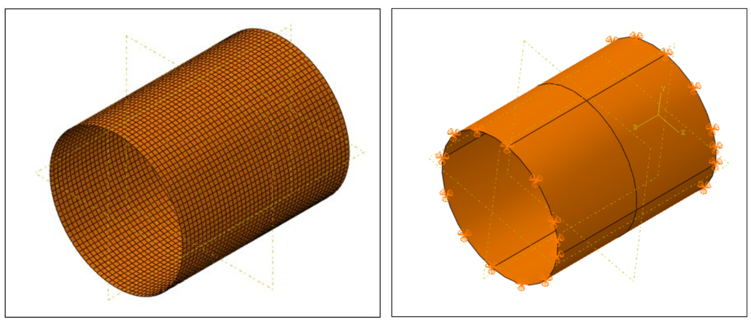

(a) (b)

Fig. 3: (a) Meshing, and (b) boundary condition of the cylindrical shell

Fig. 4 (a), and (b) illustrate the deformation and stress distribution of cylindrical steel shells under external pressure. The total number of lobes in the shell is given in Fig. 5.

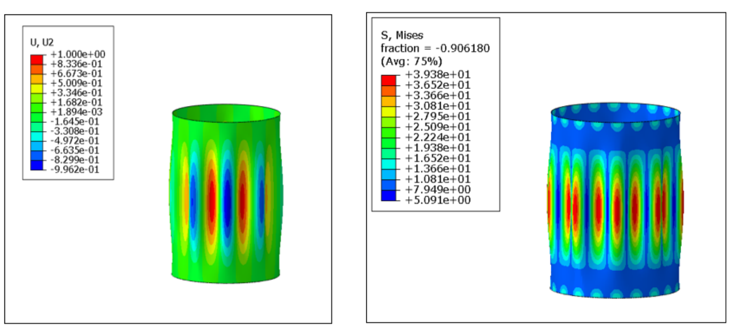

(a) (b)

Figure 4 (a): Deformed shape and (b): Max. von mises stresses of perfect cylindrical shell

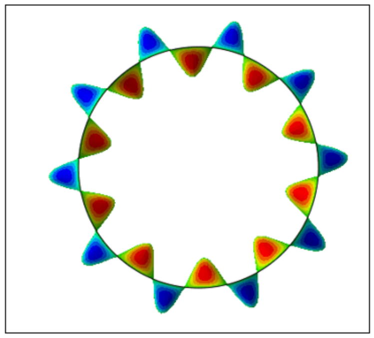

Figure 5: Number of lobes in cylindrical shell obtained from FEA = 10

The FE result are compared with theoretical calculations obtained from Jawad and Ross theory [10]. Based on the Jawad and Ross theory for buckling prediction, the top and bottom of the externally pressurized cylindrical shell are assumed to be simply supported with axial restrain. Equations 1 and 2 are classical buckling formula and are given below.

Jawad and Ross classic buckling equation 1-2;

$$P_j = \frac{0.92E \times \left(\frac{t}{R}\right)^{2.5}}{\frac{h_c}{R}} \quad (1)$$

$$P_R = \frac{2.6E\left(\frac{t}{2R}\right)^{2.5}}{\frac{h_c}{2R} - 0.45\left(\frac{t}{2R}\right)^{0.5}} \quad (2)$$

$$n = 2 \cdot 74\sqrt{\frac{R}{h_c}\sqrt{R/t}} \quad (3)$$

In the above equations, E = modulus of elasticity, t represents shell thickness, and R and h_c show the radius and height of the cylindrical shell respectively. The approximate number of waves is calculated by using Teng et al., [11] equation 3 given below. The FEA, test results, and theoretical solution for buckling pressure are given in Table 2.

Table 2: Comparisons of buckling prediction form FE, test and theory

Nature of the specimen	Analysis method	Buckling pressure (MPa)
Perfect model	FEA	0.0204
	Test result	0.0184
	Jawad theory	0.0136
	Ross theory	0.0137

2.2. CFRP Cylindrical Shells

The experimental test results conducted by Bisagni [12] are considered for numerical investigation to check the accuracy of the FEA using ABAQUS software. The specimens were four-ply laminated cylindrical composite shells and were fabricated from the Carbon Fiber Reinforced Plastic (CFRP) laminates. The specimens were 700 mm long, 1.32 mm thick and the radius-to-thickness (R/t) ratio was about 265. Table 3 presents the mechanical properties of the CFRP ply.

Table 3: Mechanical properties of the CFRP ply

Mechanical Properties	Numerical Value (MPa)
Elastic Modulus (E_{11})	52000
Elastic Modulus (E_{22})	52000
Shear Modulus (G_{12})	2350
Poisson's Ratio (v_{12})	0.3
Thickness in (mm)	0.33

Proper mesh sizes of 15 mm, 10 mm, and 5 mm with S4R shell elements are used to investigate the variation in the buckling load. Based on the mesh sensitivity study, a 5 mm mesh size is adopted for linear buckling analysis. The S4R shell elements have four nodes and a total of 6 degrees of freedom at each node, three of them are translations along the nodal direction and the remaining three are the rotations about nodal axes. The loading (shell edge) and fixed boundary conditions (BCs) are used at the base as well as at the top except for free axial translation in the loading direction. Figure 6 (a) and (b) illustrates the loading and BCs of the composite cylindrical shell respectively.

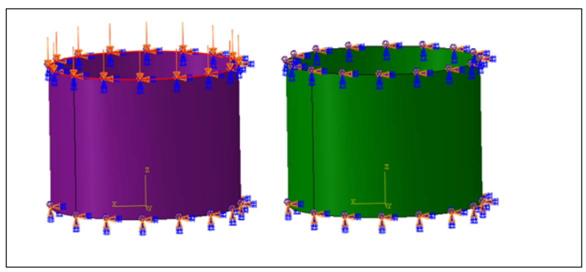

(a) (b)

Fig. 6: (a) The loading profile, and (b) BCs of the composite cylindrical shell

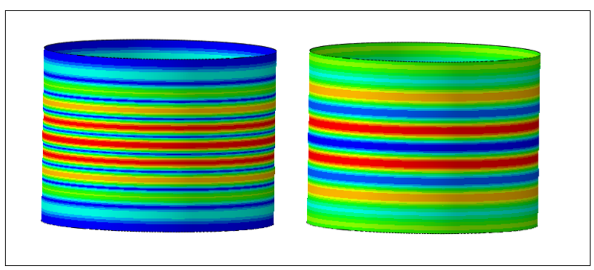

(a) (b)

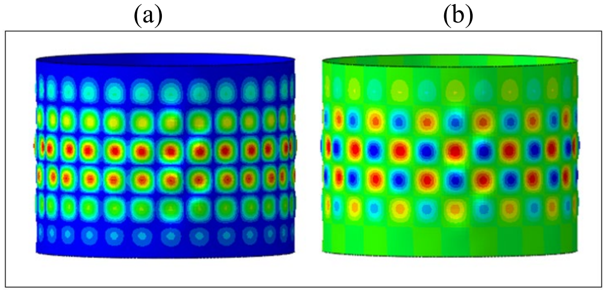

(c) (d)

Fig. 7: (a, c) Deformation of Model-1 and Model-2, (b, d) Stress distribution of composite Model-1 and Model-2 respectively.

The buckling load obtained from the linear (Eigenvalue) buckling analysis are little bit higher than the experimental buckling load and closer to the analytical result. The higher buckling load from Eigenvalue analysis is because of the nature of the cylindrical shell. The buckling load obtained from linear (Eigenvalue) analysis, Nonlinear buckling analytical result and the experimental buckling load of both composite CFRP shells are compared and presented in Table

Table 4: Comparison of numerical and experimental buckling load

Method of Analysis	Buckling Load (KN)	
	Model-1	Model-2
Linear Buckling Analysis	120.07	248.18
Nonlinear (Riks) Buckling Analysis	111.69	241.31
Experimental Analysis	112.94	161.22
Analytical Results	118.58	240.00

Similarly, the buckling load for both Model-1 and 2 are calculated using Nonlinear (Riks) buckling analysis. The buckling load obtained from the Nonlinear buckling analysis for Model-1 is very close to the experimental buckling load and slightly smaller (5.8%) than the analytical buckling load. Furthermore, the buckling load obtained from linear and Nonlinear buckling analysis for Model 2 is higher than the experimental buckling load and close to the analytical solution.

2.3. Non-linear buckling Analysis

The non-linear static Riks analysis is performed to evaluate the buckling response of the composite cylindrical shell. The two numerical models with different lay-up orientations 45/-45, 45/-45, and 0/+45, -45/0 are introduced in the ABAQUS.

The Nonlinear buckling analysis of both numerical models is performed by employing edge shell loading at the top of the cylindrical shell. The BCs are the same as in linear (Eigenvalue) buckling analysis. The different mesh sizes such as 15 mm, 10 mm, and 5 mm are used and the effect on variation in buckling load is examined. Based on the mesh convergence study, a 5 mm mesh size is adopted for both numerical models. The buckling loads for both model 1 and 2 obtained from Nonlinear buckling analysis are compared with the linear eigenvalue buckling analysis as well as with the analytical results shown in Table 5. The location of maximum deformation and circumferential stresses for both model 1 and 2 are illustrated in Figure 8 and 9 (a) and (b).

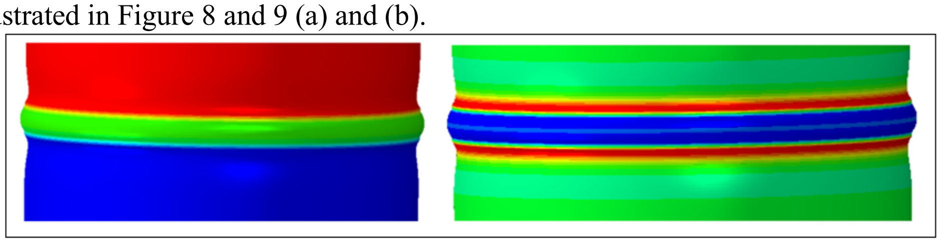

(a) (b)

Fig. 8: (a) Maximum deformation and (b) Circumferential stresses

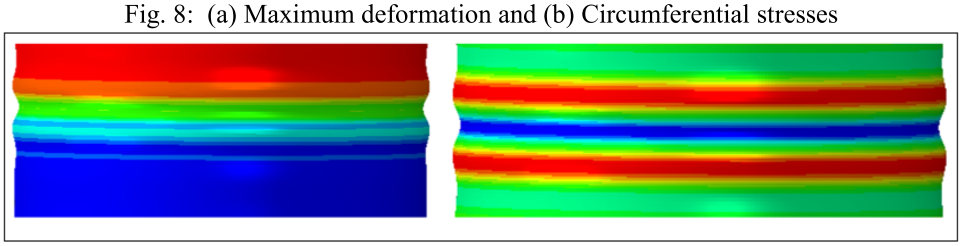

(c) (d)

Figure 9 (a): Maximum deformation and (b): Circumferential stresses

3. Hydrostatic Analysis of Cylindrical Tanks

The hydrostatic analysis of two different liquid-filled (90% and 70%) cylindrical storage tanks are presented and their their geometric and material specifications are Height, H=12.2m, and Radius is 15.20m and 12.20m with thickness t=0.025m. t=0.025m. the modulus of elasticity E=210 GPa and the Poison's ratio is 0.29. 50 mm mesh size was used for both tank models and fixed boundary conditions were applied at the base of the tanks. Figs. 10 and 11(a), (b), and (c), (d) show the the deformation response and maximum von-mises stress distribution of the tank models filled with 90% and 70% liquid respectively.

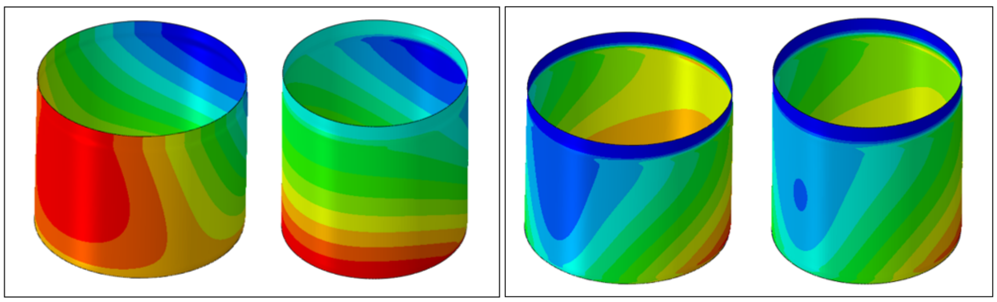

(a) (b) (c) (d)

Fig. 10: (a), (b): Deformation response of Tank-A and Tank-B, and (c), (d): Max. Von-mises stresses of Tank-A and Tank-B respectively

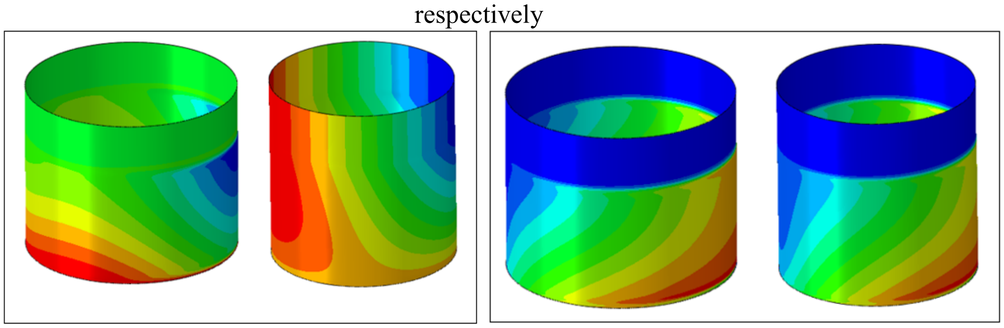

(a) (b) (c) (d)

Fig. 11 (a), (b): Deformation response of Tank-A and Tank-B, and (c), (d): Max. Von-mises stresses of Tank-A and Tank-B respectively

The deformation and stress distribution of cylindrical tank models concerning liquid levels are given in Tables 5 and 6.

Table 5: Deformation and stress variation of storage Tank filled = 90%

S. No	Tank Models	Deformation in (mm)	Von-mises stresses (MPa)	Hoop stresses (MPa)
01	Tank-A	51.36	93.44	74.01
02	Tank-B	40.88	78.70	34.86

Table 6: Deformation and stress variation of storage Tank filled = 70%

S. No	Tank Models	Deformation in (mm)	Von-mises stresses (MPa)	Hoop stresses (MPa)
01	Tank-A	14.09	24.03	19.87
02	Tank-B	10.82	19.04	14.76

4. Conclusion

This study utilizes FEA ABAQUS software to investigate the buckling behavior of cylindrical steel shells subjected static loading. The buckling pressures derived from FEA closely correspond to both experimental findings (with a 9.80% variance) and theoretical predictions. For CFRP composite cylindrical model-1, the deviation between FEA results and experimental data is a mere 5.93%, with only a 1.25% difference compared to theoretical calculations. Similarly, in model 2, FEA values closely align with theoretical expectations, whereas experimental results fall slightly lower. The buckling load obtained from linear and nonlinear buckling analyses for Model 2 surpasses the experimental buckling load and approximates the analytical solution. FEA predicts 10 waves, while theoretical equations indicate a total of 8 waves. Moreover, hydrostatic analysis of cylindrical tanks at two different liquid levels (70% and 90%) is conducted to assess stress and deformation responses. The findings suggest that reducing liquid levels significantly diminishes deformation and hoop stresses within the tanks. The highest stresses are observed at the base of the tank model due to increased liquid pressure at the bottom.

References

[1] S. Ullah and I. H. P. Mamaghani, "Numerical investigation on buckling response of cylindrical steel storage tanks under seismic excitation," *Proceedings in civil engineering*, Sep. 2023, vol. 6, no. 5, pp. 343–347.

[2] S.-E. Kim and C.-S. Kim, "Buckling strength of the cylindrical shell and tank subjected to axially compressive loads," Thin-Walled Structures, vol. 40, no. 4, pp. 329–353, Apr. 2002.

[3] M. A. Haroun and M. A. Al-Kashif, "Methodology for design of earthquake resistant steel liquid storage tanks," *WIT* Transactions on The Built Environment, vol. 81, p. 10, 2005.

[4] N. Buratti, "Seismic response of tank-fluid systems: state of the art review and dynamic buckling analysis of a steel tank with the added mass method," Masters Thesis, Dept. Civ. Eng. Università degli Studi di Bologna, Bologna, Italy, 2010.

[5] F. Tabish and I. H. P. Mamaghani, "Buckling analysis of cylindrical steel fuel storage tanks under static forces," presented at the *7th International Conference on Civil, Structural and Transportation Engineering,* Jun. 2022.

[6] F. Tabish and I. H. P. Mamaghani, "Numerical buckling behavior of perfect and imperfect steel cylinders under external pressure," in *Proceedings of International Structural Engineering and Construction*, Aug. 2023, vol. 10, no. 1.

[7] S. Aghajari, K. Abedi, and H. Showkati, "Buckling and post-buckling behavior of thin-walled cylindrical steel shells with varying thickness subjected to uniform external pressure," Thin-Walled Structures, vol. 44, no. 8, pp. 904–909, Aug. 2006.

[8] P. Wang, X. Zhu, M. Liu, and Y. Li, "Buckling behaviors and simplified design method for steel silos under locally distributed axial load," Journal of Constructional Steel Research, vol. 134, pp. 114–134, Jul. 2017.

[9] J. B. Greenberg and Y. Stavsky, "Buckling of composite orthotropic cylindrical shells under non-uniform axial loads," Composite Structures, vol. 30, no. 4, pp. 399–406, Jan. 1995.

[10] F. M. Aydın Korucuk, M. Maali, M. Kılıç, and A. C. Aydın, "Experimental analysis of the effect of dent variation on the buckling capacity of thin-walled cylindrical shells," Thin-Walled Structures, vol. 143, p. 106259, Oct. 2019.

[11] J. G. Teng, Y. Zhao, and L. Lam, "Techniques for buckling experiments on steel silo transition junctions," Thin-Walled Structures, vol. 39, no. 8, pp. 685–707, Aug. 2001.

[12] C. Bisagni, "Experimental buckling of thin composite cylinders in compression," AIAA Journal, vol. 37, no. 2, pp. 276–278, Feb. 1999.